BBA - Molecular Basis of Disease 1865 (2019) 308–321

Contents lists available at ScienceDirect

BBA - Molecular Basis of Disease

journal homepage: www.elsevier.com/locate/bbadis

Pharmacologic IL-6Rα inhibition in cholangiocarcinoma promotes cancer cell growth and survival

Florian Kleinegger[a], Eva Hofer[a], Christina Wodlej[a,b], Nicole Golob-Schwarzl[a,b], Anna Maria Birkl-Toeglhofer[a], Alexander Stallinger[c], Johannes Petzold[a], Anna Orlova[d,e], Stefanie Krassnig[a], Robert Reihs[a], Tobias Niedrist[f], Harald Mangge[f], Young Nyun Park[g], Michael Thalhammer[h], Ariane Aigelsreiter[a], Sigurd Lax[i], Christoph Garbers[j], Peter Fickert[k], Stefan Rose-John[j], Richard Moriggl[d,e,l], Beate Rinner[c], Johannes Haybaeck[a,b,m,*]

[a] Diagnostic & Research Center for Molecular BioMedicine, Institute of Pathology, Medical University of Graz, Austria
[b] Center for Biomarker Research in Medicine, Graz, Austria
[c] Department for Biomedical Research, Core Facility Alternative Biomodels and Preclinical Imaging, Medical University of Graz, Austria
[d] Ludwig Boltzmann Institute for Cancer Research, Vienna, Austria
[e] Institute of Animal Breeding and Genetics, University of Veterinary Medicine Vienna, Austria
[f] Clinical Institute of Medical and Chemical Laboratory Diagnostics, Medical University of Graz, Austria
[g] Department of Pathology, Brain Korea 21 PLUS Project for Medical Science, Yonsei University College of Medicine, Seoul, South Korea
[h] Department of General Surgery, Medical University of Graz, Austria
[i] Department of Pathology, Hospital Graz South-West, Austria
[j] Institute of Biochemistry, Kiel University, Germany
[k] Division of Gastroenterology and Hepatology, Medical University Graz, Austria
[l] Medical University of Vienna, Austria
[m] Department of Pathology, Medical Faculty, Otto von Guericke University Magdeburg, Germany

ARTICLE INFO

Keywords:
IL-6 receptor signaling
IL-6 trans-signaling
Cholangiocarcinoma
Gallbladder cancer
STAT3

ABSTRACT

Biliary tract cancer (BTC) represents a malignant tumor of the biliary tract including cholangiocarcinoma (CCA) and the carcinoma of the gallbladder (GBC) with a 5-year survival rate between 5 and 18% due to late diagnosis and rapid disease progression. Chronic inflammation is one of the main risk factors for CCA and GBC in particular. IL-6, as a mediator of inflammation, can act through a membrane-bound receptor alpha-chain (mIL-6R, "IL-6 classic signaling") or *via* soluble forms (sIL-6R, "IL-6 trans-signaling"). However, little is known about the impact on cellular responses of IL-6 trans-signaling on BTC. We analyzed primary tumors as whole sections and as tissue microarrays, and also searched The Cancer Genome Atlas database. Compared to non-neoplastic, non-inflamed gallbladder tissue, IL-6Rα was downregulated in GBC, and this correlated with the patients' overall survival. Furthermore, different CCA cell lines and compounds for activation (IL-6 and Hyper-IL-6) or inhibition (Tocilizumab and sgp130Fc) of IL-6 classic signaling and trans-signaling were used to determine their effects on cellular processes between the two modes of IL-6 signaling. Inhibition of IL-6 trans-signaling by sgp130Fc reduced CCA cell line viability and apoptosis, whereas migration and proliferation were increased. We conclude that IL-6Rα expression is a good prognostic marker for GBC, and that the blocking of IL-6 trans-signaling and activation of IL-6 classic signaling have tumor promoting activity. These findings warrant the exclusion of patients with GBC or other malignancies associated with bile metabolism from IL-6R inhibitor therapy.

1. Introduction

Biliary tract caner (BTC) is a malignant gastrointestinal neoplasm originating from the entire biliary tree. The major function of the bile ducts is to move hepatic bile from the liver and gallbladder to the small intestine, where bile is essential to the transport and metabolization of fat. BTC is classified by anatomic location in intrahepatic cholangiocarcinoma (iCCA), extrahepatic perihilar CCA (pCCA), distal CCA (dCCA) and gallbladder cancer (GBC) [1]. Although GBC and CCA differ in terms of incidences, age and gender, and risk factors, chronic

* Corresponding author at: Department of Pathology, Otto von Guericke University Magdeburg, Leipziger Str. 44, D-39120 Magdeburg, Germany.
E-mail address: johannes.haybaeck@med.ovgu.de (J. Haybaeck).

https://doi.org/10.1016/j.bbadis.2018.11.006
Received 21 June 2018; Received in revised form 25 October 2018; Accepted 7 November 2018
Available online 09 November 2018

inflammation represents one of the most common key mechanisms of BTC development [2–4]. CCA forms heterogeneous group of malignancies featuring biliary tract differentiation. CCA is the second most common primary liver tumor and accounts for approximately 10–15% of all hepatobiliary malignancies. The development of CCA is linked to a wide spectrum of conditions such as cholestasis and inflammation of the liver and the biliary tract, with noticeable increasing incidences worldwide. BTC has high mortality owing to its aggressiveness, late diagnosis and refractory nature. Further risk factors for BTC are age, ethnicity, obesity and metabolic syndrome, liver cirrhosis, hepatitis, smoking, alcohol abuse, chronic stress and bile duct abnormalities [4]. The latter are often inborn defects causing choledochal cysts which promote dilated and irregular bile ducts. Several risk factors can be prevented whereas others are beyond preventive controls.

IL-6 is a major mediator of inflammation and trauma situations in infected patients where upon blockade it can reduce fever and the cytokine storm associated with it. However, IL-6 is also a pleiotropic cytokine involved in wound healing or in differentiation (*e.g.* B-cell and T-cell subsets), and it can have beneficial effects if not strongly and chronically stimulated. IL-6 is a dimer that interacts with IL-6Rα chain (CD126, gp80) on the cell membrane ("IL-6 classic signaling") and the long signaling chain in a hexameric complex [5]. The ligand-receptor complex is not able to transduce signals directly, but tyrosine kinases of the JAK family (*i.e.* JAK1, JAK2, TYK2) promote IL-6 signal transduction through tyrosine phosphorylation of gp130 and other important substrate phosphorylations. Among these, the most important substrate downstream of JAK kinases action is STAT3 tyrosine phosphorylation, which results in parallel dimerization of the molecules and translocation into the nucleus or mitochondria. Oncogenic STAT3 is critically balanced by the tumor suppressor protein STAT1, which was proven to correlate with the degree of inflammation in pre-cancerous lesions of CCA [6–10]. Epithelial cell types, such as hepatocytes or biliary epithelial cells, but also neutrophils, macrophages or lymphocytes, express IL-6Rα [11]. However, IL-6 has also been shown to impact cells lacking IL-6Rα. This mechanism is mediated by soluble forms of IL-6Rα (sIL-6R) and was termed IL-6 trans-signaling [12]. Solubilization of the IL-6Rα is caused either by alternative splicing or proteolytic cleavage of the membrane-bound form (mIL-6R) by the metalloproteinase ADAM17, which is often persistently expressed in cancer cells [13–16].

In a small cohort, an IL-6Rα polymorphism was shown to be associated with a higher risk of CCA [17] and permanent IL-6/STAT3 signaling was proven in CCA [10,18]. Compared to hepatocellular carcinoma, metastatic colorectal cancer and benign biliary diseases, IL-6 serum and bile levels of CCA patients were significantly increased. Moreover, a correlation between IL-6 levels and tumor burden as well as survival rates was found in CCA patients [19–22]. On a genetic level, IL-6 was proven to alter methylation at gene promotor regions of *e.g. CASP8* and *SURVIVIN*, indicating its important role in CCA cell survival [23].

It was demonstrated that IL-6 trans-signaling impacts various cancer types, such as pancreatic ductal adenocarcinoma and hepatocellular carcinoma [24,25]. In the latter it was proven, that IL-6 trans-signaling is the superior and mandatory form of IL-6 signaling for hepatocellular carcinogenesis [25]. Moreover, IL-6 trans-signaling plays a major role in acute inflammation by directing T-cell infiltration [26] and inhibition of IL-6 trans-signaling sufficiently blocked inflammatory processes in inflammatory diseases like sepsis, atherosclerosis, asthma and rheumatoid arthritis [27–30]. However, little is known about IL-6 trans-signaling in BTC.

Therefore, our investigations focused on the impact of IL-6R-mediated signaling on cellular processes in BTC. We first compared GBC tissue with non-neoplastic, non-inflamed gallbladder tissue samples regarding the expression of proteins involved in IL-6 signaling. Second, we performed *in vitro* studies to define the cellular responses of IL-6 classic signaling and trans-signaling *via* specific activation and inhibition of this pathway in different CCA cell lines.

2. Material and methods

All chemicals not mentioned otherwise were purchased from Sigma Aldrich (St. Louis, USA).

2.1. Tissue microarray

Under the approval of the ethics committee of the Medical University of Graz (28-294 ex 15/16) and the institutional review board of the Severance Hospital (no. 4-2014-0421), 428 formalin-fixed, paraffin-embedded patient samples were collected retrospectively from the Medical University of Graz (43%), the Hospital Graz South-West (6%), the Medical University of Innsbruck (11%) and the University Hospital of Seoul (40%). Samples of the Medical University of Graz were provided by the Biobank Graz. Tissue cones of 0.6 mm in diameter were punched out from the tumor area and embedded as tissue microarray (TMA) in a fresh paraffin block (Beechers Instruments, Sun Prairie, USA). A detailed description of the patient cohort was reported previously [31].

2.2. Immunohistochemistry

TMAs were cut in 3 μm thick sections, and antigen retrieval was performed either with 0.01 M citrate buffer (pH 6) or 1 mM Tris-EDTA buffer (pH 9). Primary antibody (Suppl. Table 1) was incubated overnight at 4 °C. The detection was performed using the Super Stain System-HRP AEC detection kit (Empire Genomics, Buffalo, USA). TMAs were evaluated by two independent blinded observers (J.H., E.H.). Staining intensity was scored as follows: no (score = 0), weak (score = 1), moderate (score = 2) and strong (score = 3) staining. No and weak staining intensity was further grouped as low expression, whereas high expression was represented by moderate and strong staining intensity.

2.3. Survival analysis

Kaplan-Meier analysis was done using the R survival package. Statistical analysis of the TMA data was performed with the Cox proportional hazards regression model using the Likelihood ratio test. The *in silico* analysis of the Cancer Genome Atlas (TCGA) dataset (http://cancergenome.nih.gov/), including 28 CCA patients, was done using gene expression data, stratified by median expression to identify the association between *IL-6Rα* gene expression and overall survival using the log-rank test. Statistically significance was assumed at $p < 0.05$.

2.4. Protein isolation and immunoblot

A detailed description of the method is reported elsewhere [32]. In short, cells were scraped and lysed in Nonidet P-40 lysis buffer (0.05 M Tris-HCl, 5 mM NaCl, 0.5% NP-40, 0.1 mM Pefabloc, 1 mM DTT, cOmplete Mini and PhosSTOP). Tissues were homogenized using MagNA Lyser homogenizer (Roche Diagnostics, Risch-Rotkreuz, Switzerland). 30 μg of total protein lysate were loaded onto a SDS polyacrylamide gel (30% Acrylamide/Bis-acrylamide solution; ROTH, Karlsruhe, Germany). Primary antibodies used are listed in Suppl. Table 1 and were incubated at 4 °C overnight. Proteins were visualized using the chemiluminescence Amersham ECL Prime Western Blotting Detection Reagent (GE Healthcare Life Science, Buckinghamshire, UK) and exposed in the Image Quant LAS 500 (GE Healthcare, Buckinghamshire, UK). For trichloracetic acid (TCA) precipitation, the cell culture supernatants were collected, and TCA was added to a final concentration of 10% and incubated overnight at −20 °C.

2.5. Quantitative Real-Time PCR

Total RNA was isolated using TRIzol® reagent (Life Technologies;

Woolston, UK) with subsequent phenol-chloroform extraction and is described in detail elsewhere [33]. Briefly, cell lines and frozen tissues were lysed, and 1 μg of RNA was reversely transcribed to cDNA using the High-Capacity cDNA Reverse Transcription Kit (Applied Biosystems, Foster City, USA). To determine gene expression, the Power SYBR Green PCR Master Mix Kit (Applied Biosystems, Foster City, USA), 5 ng cDNA, and 5 μM primers were used in a QuantStudio™ 7 Flex Real-Time PCR System (Applied Biosystems, Foster City, USA). Primers are listed in Suppl. Table 2. GAPDH was determined by NormFinder [34] to be the most stable endogenous control. The relative gene expression levels were calculated using the $2^{\Delta\Delta CT}$ method [35].

2.6. Cell culture and compounds

The cell lines TFK-1 and EGI-1 were a kind gift from Prof. Kai Breuhahn (University Hospital of Heidelberg, Germany) and cultivated as described elsewhere [36]. Mz-ChA-1, Mz-ChA-2 and SK-ChA-1 were kindly provided by Prof. Alexander Knuth (University of Zurich, Switzerland) and cultured in RPMI-1640 (Gibco, Life Technologies, Darmstadt, Germany) supplemented with 10% FBS (Gibco, Life Technologies, Darmstadt, Germany), L-Glutamine (2 mM), MEM non-essential amino acids (1× Gibco, Life Technologies, Darmstadt, Germany) and penicillin (100 U/mL)/streptomycin (100 μg/mL). All cell lines were maintained at 37 °C in a humid atmosphere with 5% CO_2, routinely tested for *mycoplasma* contamination (PCR Mycoplasma Kit, Promocell GmbH, Heidelberg, Germany), and STR-profiling (PowerPlex 16HS System, Promega, Madison USA) was done to verify cell lines.

Hyper-IL-6, a fusion protein of IL-6 and sIL-6R that mimics IL-6 trans-signaling, and sgp130Fc, a protein that specifically blocks IL-6 trans-signaling, were produced as described previously [37–40]. Human recombinant IL-6 was purchased from Peprotech (Rocky Hill, USA). Tocilizumab (RoActemra®), an IL-6Rα inhibitor, was purchased from Roche Diagnostics (Risch-Rotkreuz, Switzerland).

2.7. Immunofluorescence staining

Cell lines were seeded on sterile Flex IHC microscope slides (Dako, Agilent Santa Clara, USA) and allowed to adhere overnight. After methanol fixation, cells were permeabilized with 1% Triton X-100 (Sigma-Aldrich, St. Louis, USA). Blocking was performed with 5% horse serum (ThermoFischer Scientific, Massachusetts, USA). Samples were incubated with primary antibody (mouse anti-human IL-6Rα (4–11), 4 μg/mL [55]) overnight at 4 °C. Secondary antibody (AlexaFluor®488 goat anti-mouse IgG, Invitrogen ThermoFischer Scientific, Massachusetts, USA; 1:500) was used according to the manufacturer's protocol. Counterstaining was done with 4′,6-Diamidin-2-phenylindol (DAPI, Sigma Life Science, St. Louis, USA), and pictures were taken with a Zeiss LSM 510 Meta microscope (Oberkochen, Germany).

2.8. Surface staining of IL-6Rα

Cells were grown under standard conditions and detached with 10 mM EDTA in PBS. Samples were incubated in blocking buffer (10% FBS + 0.1% NaN_3) and resuspended in Cell Staining Buffer (BioLegend, San Diego, USA). Staining was performed with APC anti-human CD126 antibody (BioLegend, San Diego, USA) and APC mouse IgG1, κ isotype control (BioLegend, San Diego, USA). Measurement was performed with a CytoFLEX S (Beckman Coulter, Brea, USA) flow cytometer using CytExpert software (Beckman Coulter).

2.9. Electrochemiluminescence immunoassay (ECLIA)

Cells were seeded in 6-well plates and allowed to adhere overnight. After serum starvation, the cells were cultivated in serum-free medium for 24 h. The cell culture supernatant was collected and stored at −80 °C prior to analysis. The amount of IL-6 was determined using the COBAS® immunoassay system (Roche Diagnostics, Risch-Rotkreuz, Switzerland). Calibration was performed using the CalSet IL-6 Elecsys® (Roche Diagnostics, Risch-Rotkreuz, Switzerland). Each assay was performed in three independent experiments.

2.10. Cell viability

Between 1 and 5×10^4 cells/well were seeded into 96-well plates and allowed to adhere for 24 h. Cells were serum-starved overnight and treated for 24 h, 48 h and 72 h with different concentrations of the compounds under serum-free conditions. Viable cells were analyzed by the mitochondrial reduction of 3-(4,5-dimethylthiazol-2-yl)-2,5-diphenyltetrazolium bromide (MTT, Sigma Aldrich, Missouri, USA) to (*E*,*Z*)-5-(4,5-dimethylthioazol-2-yl)-1,3-diphenylfromazan. Cells were incubated with 5.5 mg/mL MTT for 2 h at 37 °C. The supernatant was discarded, and cells were lysed with 3% SDS for 15 min at room temperature. The formazan crystals were dissolved in 4 mM isopropanol/HCl under vigorous shaking. Absorption was measured at 570 nm (Synergy™ 4, BioTek, Winooski, USA). Each assay was performed in three independent experiments.

2.11. Proliferation assay

The xCELLigence DP device (OLS Omni Life Science, Bremen, Germany) was used to determine real-time cell proliferation. After background measurement, 5×10^3 cells/well were seeded into electronic microtiter plates (E-Plate™, OLS Omni Life Science, Bremen, Germany) and allowed to adhere for 24 h. Afterwards, serum starvation took place for 24 h, followed by treatment of the compounds under serum free conditions. Cell density was measured every 20 min for 72 h. Normalization was done directly after treatment, and the slope of the growth curve and the population doubling time (PDT) were calculated using RTCA software version 2.0 (ACEA Biosciences, Inc., San Diego, USA). Each assay was performed in three independent experiments.

2.12. Apoptosis assay

Between 1 and 5×10^4 cells/well were seeded into clear bottom black 96-well plates and allowed to adhere, followed by serum starvation overnight. Apoptotic cells were analyzed using YoPro©-1 iodide (491/509) (Thermo Fisher Scientific, Massachusetts, USA) after 24 h, 48 h and 72 h of treatment with Hyper-IL-6 (5 ng/mL, 15 ng/mL and 30 ng/mL), IL-6 (15 ng/mL, 50 ng/mL and 100 ng/mL), Tocilizumab (1 μg/mL, 10 μg/mL and 25 μg/mL) and sgp130Fc (1 μg/mL, 10 μg/mL and 25 μg/mL). The supernatant was removed, and fluorescence (485/528 nm) was measured (Synergy™ 4, BioTek, Winooski, USA). Each assay was performed in three independent experiments.

2.13. Wound healing assay

Cells were grown in 6-well plates to 100% confluency. After 24 h serum starvation, the cell layer was scratched with a 200 μL tip and treated with 15 ng/mL Hyper-IL-6, 100 ng/mL IL-6, 25 μg/mL Tocilizumab, 25 μg/mL sgp130Fc or in combination. Pictures were taken with an Olympus Inverse IX53 microscope after 24 h, 48 h and 72 h. Wound closure was calculated using the TScratch software version 1.0 [41]. Each assay was performed in three independent experiments.

2.14. Cell cycle analysis

Cells were grown and treated with Hyper-IL-6 (15 ng/mL), IL-6 (100 ng/mL), Tocilizumab (25 μg/mL) and sgp130Fc (25 μg/mL) for 72 h under serum-starved conditions, detached using Trypsin (Gibco, Life Technologies, Darmstadt, Germany), washed with PBS, and resuspended in hypotonic propidium iodide (PI) lysis buffer (0,1% sodium citrate, 0,1% Triton-X, 100 μg/mL RNAseA and 50 μg/mL PI).

Table 1
Clinicopathological characteristics of patient derived tissue.

	Frozen tissue (n = 26)		TMA (n = 428)	
	GBC (n = 14)	NNT (n = 12)	GBC (n = 367)	NNT (n = 61)
Age (± SD)	70.4 (8.5)	57.8 (8.1)	68.8 (10.7)	64.2 (9.6)
Gender				
Female	9	2	268	36
Male	5	10	99	25
Subtype				
Adenocarcinoma	14		336	
Adenosquamous	4		13	
Tubulary	4		77	
Mucinous	1		6	
Tubulo-papillary	4		25	
Mixed	1		32	
Papillary	0		11	
Solid	0		7	
Unknown	0		165	
Squamous cell carcinoma	0		6	
Without subtyping	0		25	
Grading				
Low	7		221	
High	6		137	
Unknown	1		9	

Samples were measured on a BD LSRII (BD Bioscience, Brea, CA, USA) flow cytometer, and cell cycle analysis was performed with the Modefit software version 5.0 (Verity Software House, Topsham, USA). Each assay was performed in three independent experiments.

2.15. Statistical analysis

If not mentioned differently, statistical analysis was performed with GraphPad Prism version 5.01. The statistical test (*t*-test, Mann-Whitney *U* test, one-way ANOVA) was selected regarding the data distribution of each experiment.

3. Results

3.1. High IL-6Rα expression correlates with better overall survival in gallbladder cancer patients independent of grade and gender

TMA slides of 367 patients suffering from GBC and 61 non-inflamed, non-neoplastic gallbladders (NNT) were examined to address the prognostic potential of the IL-6Rα. The patients' characteristics are summarized in Table 1. Expression of the IL-6Rα was evaluated by immunohistochemistry based on staining intensity. Positive immunoreactivity was seen as clear cytosolic/membranous staining of GBC tissue (Fig. 1A). In total, 365 (99.4%) patients showed positive immunoreactivity, whereas no significant staining was visible in two patients (*i.e.* 0.6%). IL-6Rα expression was strong in 305 (83.1%) samples and weak in 60 (16.3%). Patients with high IL-6Rα expression levels showed a significantly better survival probability than those with low expression ($p < 0.001$, Fig. 1B). A comparable finding was observed when GBC samples were subdivided into a high and low grade group ($p < 0.001$, Fig. 1C), whereas no differences were observed when differentiated by gender ($p > 0.9$, Fig. 1D). Computational analysis of the TCGA database revealed similar results, based on *IL-6Rα* gene expression of 28 Caucasian patients suffering from known primary CCA (Fig. 1E). These findings suggest IL-6Rα might serve as a novel prognostic marker for GBC patients' overall survival. To address downstream signaling of the IL-6Rα, snap-frozen GBC tissue was analyzed on protein and RNA level.

3.2. Downregulation of IL-6α and decreased STAT3 tyrosine phosphorylation are found in GBC in fresh frozen tissue

IL-6Rα expression and IL-6 signaling are often strong in carcinomas. Therefore, we analyzed proteins involved in IL-6R mediated signaling on mRNA and protein level in snap frozen tissue.

On mRNA level, expression analysis of *IL-6Rα* revealed a significant ($p < 0.05$) downregulation in GBC compared to NNT (Fig. 2A). *STAT3* gene expression was significantly ($p < 0.05$) upregulated (Fig. 2B). No significant effect between the two groups was found for the tyrosine kinases *JAK1* (Fig. 2C), *JAK2* (Fig. 2D), *TYK2* (Fig. 2E) and *ADAM17* (Fig. 2F).

Comparison of 12 NTT and 14 GBC tissue samples by immunoblotting (Fig. 2G) proved decreased expression of both IL-6R forms on protein level, with stronger effects on mIL-6R ($p < 0.05$). A significant ($p < 0.001$) downregulation of the IL-6Rα in GBC (Fig. 2H–J) was observed after densitometric analysis. STAT3 tyrosine phosphorylation was downregulated, but was still present in GBC, whereas STAT3 was significantly ($p < 0.001$) downregulated. A calculation of the ratio between p-STAT3 (Tyr705) and STAT3 produced a slight but not significant downregulation in GBC (Fig. 2K–M).

3.3. Cholangiocarcinoma cell lines express key components of IL-6R mediated signaling

It has been demonstrated that liver cells express both IL-6Rα and IL-6 [42]. We proved the expression of IL-6Rα in GBC tissue, in healthy gallbladder samples (Fig. 2) and in five different CCA cell lines, *i.e.* EGI-1, TFK-1, Mz-ChA-1, Mz-ChA-2 and SK-ChA-1 (Fig. 3).

The presence of the IL-6Rα in CCA cell lines was visualized using immunofluorescence staining (Fig. 3A), and its location on the cell surface was analyzed by flow cytometry (Suppl. Fig. 1A). Furthermore, gene expression analysis revealed *IL-6Rα* expression in all tested cell lines (Fig. 3B).

Hepatic damage is known to lead to IL-6 production together with other inflammatory cytokines such as TNF-α or IL-1β. In addition, IL-6 is important for tissue remodeling *e.g.* during wound healing. Thus, we addressed the question whether cholangiocarcinoma cells themselves would be a source for IL-6 production. Surprisingly, three cell lines secreted significant amounts of IL-6 measured in their cell culture supernatant (Fig. 3C). Additionally, there were dramatic differences regarding the amount of IL-6 secreted in the supernatant of cell lines. TFK-1 cells showed the highest IL-6 concentration (143 pg/mL), which could also be a result of high STAT3 signaling in this cell line promoting IL-6 targeted gene induction, followed by EGI-1 (14 pg/mL) and Mz-ChA-1 (1 pg/mL). In contrast, no IL-6 was detectable (< 0.5 pg/mL) in the supernatant of Mz-ChA-2 and SK-ChA-1 (Fig. 3C). IL-6 production data were further confirmed by *IL-6* gene expression analysis following the same trend like protein data (Suppl. Fig. 1B). Furthermore, the soluble form of the IL-6Rα protein was found to be present in total cell lysates (Fig. 3D). Despite expression of IL-6Rα, not all cell lines secreting IL-6 in the cell culture supernatant showed phosphorylated STAT3 (Fig. 3D). SK-ChA-1 cells were found to have p-STAT3 (Tyr705) but were lacking IL-6 expression. Mutational analysis of this cell line revealed a JAK3 (C395A) mutation, which manifests in the SH2 domain of JAK3, possibly leading to an activation of STAT3 (Suppl. Table 3). Furthermore, all tested cell lines showed mutations in *TP53* and deletion of the *CDKN2A* locus. Alternative transcription factors for IL-6 synthesis are AP-1 and NFκB family members not analyzed here. To confirm soluble IL-6R shedding, we performed protein precipitation using TCA which revealed the presence of the soluble IL-6 receptor in the cell culture supernatant (Suppl. Fig. 1C).

Whole cell lysates were immunoblotted (Fig. 3D) to investigate the expression of proteins involved in IL-6/IL-6R/gp130/STAT3 signaling. All cell lines were proven to express gp130, STAT3, p-STAT3 (Ser727), and the suppressor of cytokine signaling 3 (SOCS3).

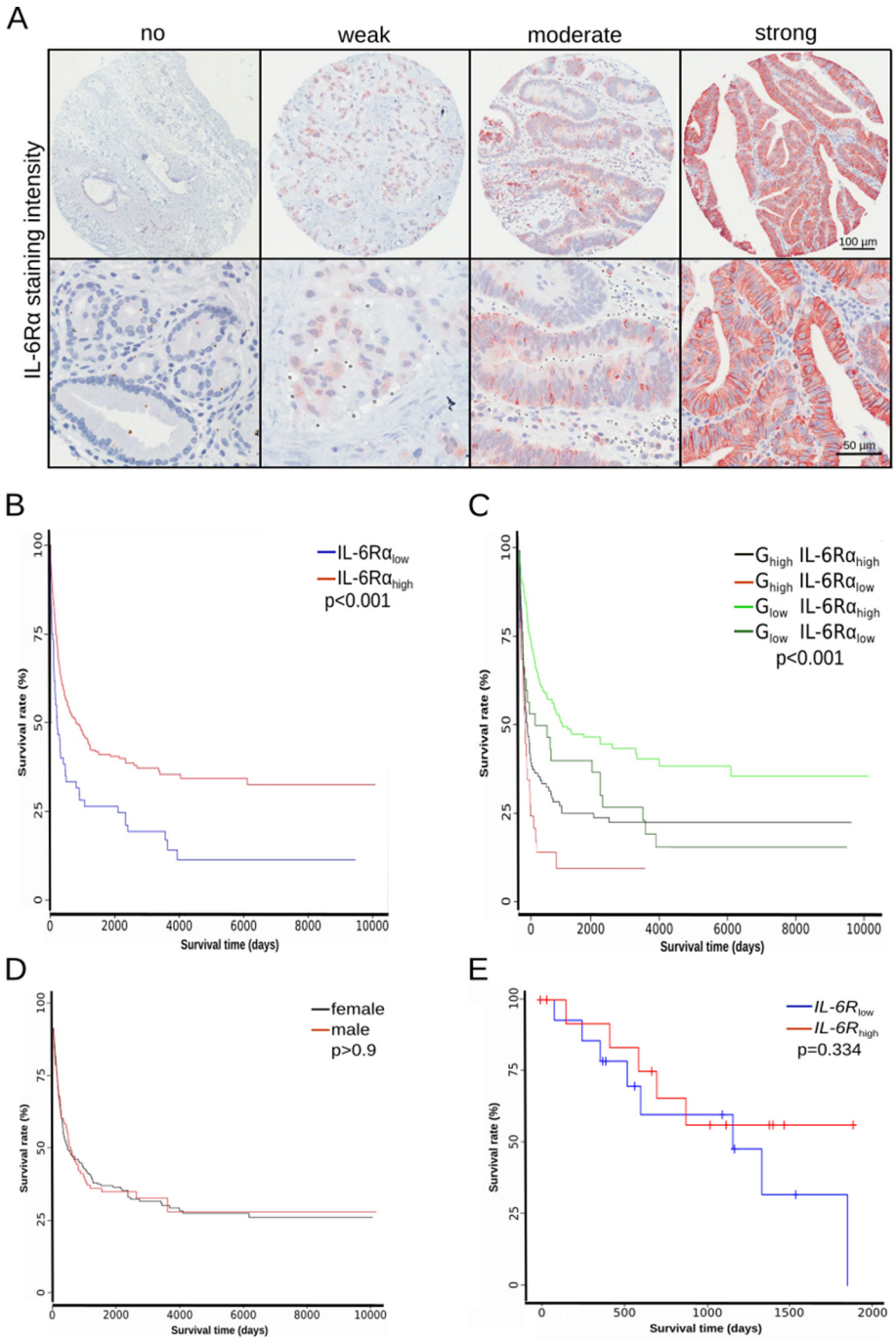

Fig. 1. Low IL-6Rα expression correlates with poor overall survival in GBC patients. (A) Representative tumor tissue microarray (TMA) areas with no, weak, moderate and strong IL-6Rα staining intensity. Scale bars: 100 µm and 50 µm. (B) Kaplan-Meier curve of IL-6Rα expression and overall survival based on TMA staining intensity (n = 367). (C) Correlation between IL-6Rα expression and high or low grade GBC patients with overall survival (n = 367). (D) TMA based survival curve of IL-6Rα staining intensity and gender of GBC patients (E) The Cancer Genome Atlas (TCGA) based, calculated correlation between *IL-6Rα* gene expression (n = 14 per group) and overall survival in Caucasians suffering from known primary CCA (n = 28).

Based on the basic characterization of CCA cell lines, we focused on Mz-ChA-2 cells as a tool to study the differences between activation by IL-6 and Hyper-IL-6, and TFK-1 as model for the inhibition of IL-6 signaling, because of their differences in IL-6 expression and pY-STAT3 activation.

3.4. Hyper-IL-6 leads to increased and persistent tyrosine phosphorylation of STAT3 efficiently blocked by sgp130Fc

To study different effects of IL-6 trans-signaling and IL-6 classic signaling on STAT3 activation in CCA, cells were incubated with 10, 25 or 50 ng/mL of IL-6 or Hyper-IL-6 and protein lysates were immunoblotted. Mz-ChA-2 cells were chosen because neither IL-6 nor tyrosine phosphorylated STAT3 were detected therein. IL-6 led to increased phosphorylation of STAT3 (Tyr705) within 1 h, which decreased over time (Fig. 4A) without affecting Ser727 phosphorylation. This finding possibly suggests an important role for mitochondrial STAT3 activity in CCA, since serine phosphorylated STAT3 is involved in ATP production through direct binding to complex 1 and 3 of the respiratory chain. Hyper-IL-6 caused a persistent and prolonged activation of STAT3 through the whole time of 24 h (Fig. 4B). Both compounds had no influence on the levels of p-STAT3 (Ser727), total STAT3, and SOCS3 as negative feedback control mechanism.

To investigate the potential inhibitory effects of Tocilizumab and sgp130Fc on the two models of IL-6 signaling, Mz-ChA-2 cells were pretreated for 6 h with the inhibitors (1, 10, 25 µg/mL) followed by an incubation of 30 min with either IL-6 (100 ng/mL) or Hyper-IL-6 (15 ng/mL). Tocilizumab blocked the IL-6 induced tyrosine 705 phosphorylation of STAT3 at a concentration of 10 µg/mL, whereas sgp130Fc had no influence on IL-6 induced STAT3 phosphorylation

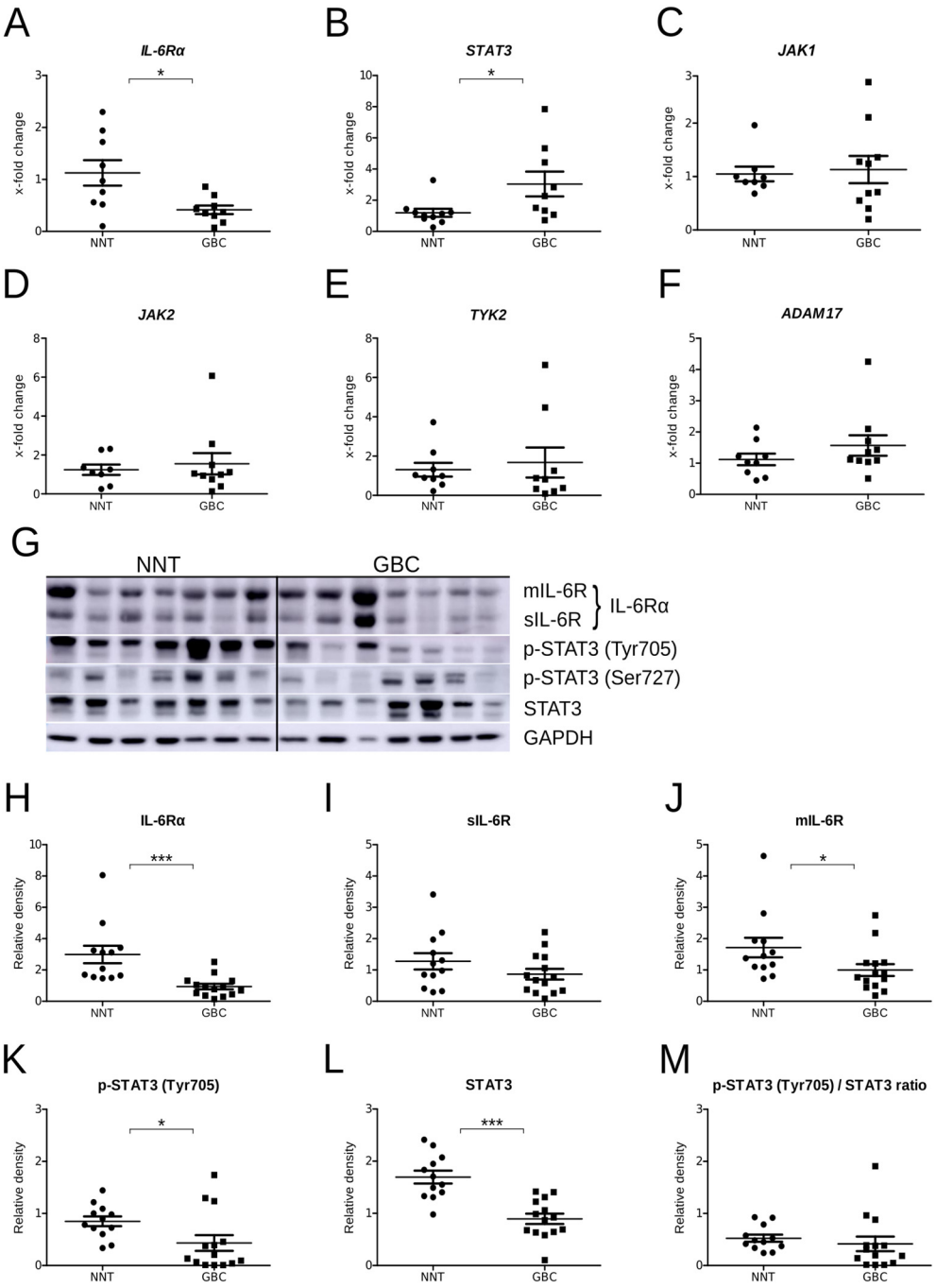

Fig. 2. GBCs express the machinery for IL-6R shedding, and the IL-6Rα is down-regulated in GBC affecting STAT3 tyrosine phosphorylation. Gene expression of (A) *IL-6Rα* (B) *STAT3* (C) *JAK1* and (D) *JAK2* (E) *TYK2* and (F) *ADAM17* was analyzed using qRT-PCR and is shown as x-fold change calculated with the ΔΔCt method. GAPDH was used as internal control. GBC (n = 9), NNT (n = 9) (G) Representative immunoblot analysis of IL-6R mediated signaling in NNT (n = 12) and GBC tissue (n = 14). Densitometrical analysis was performed using ImageJ software (NIH, Maryland, USA). (H–J) Relative density of IL-6Rα in membrane-bound (mIL-6R) and soluble (sIL-6R) form. (K-M) Relative density of STAT3 tyrosine phosphorylation, total STAT3 and their ratio of NNT compared to GBC. Bars represent mean ± SEM. Statistical analyses: t-test/Mann-Whitney *U* test, *p < 0.05, ***p < 0.001.

(Fig. 4C). Hyper-IL-6 induced STAT3 activation was blocked by 1 μg/mL sgp130Fc (Fig. 4D). As expected, Tocilizumab failed to efficiently block the activity of Hyper-IL-6 since in the Hyper-IL-6 protein, the IL-6 binding interface of the IL-6Rα is permanently engaged by IL-6 and is therefore not accessible to the antibody (Fig. 4D) [37]. Serine phosphorylated STAT3 was independent of any pharmacologic inhibition of the IL-6 receptor system.

3.5. Tocilizumab and sgp130Fc decrease constitutive active STAT3 in vitro

To investigate if blocking of IL-6R-mediated signaling decreased constitutively active STAT3, the cell line TFK-1 was chosen because of its high endogenous IL-6 levels. Cells were treated with Tocilizumab (25 μg/mL), sgp130Fc (1 μg/mL) or both for pharmacologic inhibition of the IL-6 receptor system, harvested after 24 h, 48 h and 72 h, and protein lysates were immunoblotted (Fig. 4E). Tocilizumab treatment decreased tyrosine phosphorylation by 40% after 24 h, whereas inhibition of IL-6 trans-signaling with sgp130Fc reduced STAT3 activation by 40% after 48 h. Combination of both compounds led to a stronger inhibition (60%) after 24 h, without affecting p-STAT3 (Ser727), total STAT3 and SOCS3 expression (Fig. 4F). We conclude that STAT3 tyrosine phosphorylation is a consequence of autocrine IL-6 signaling in TFK-1 cells.

3.6. Tocilizumab and sgp130Fc lead to increased cell motility

To address cell motility upon treatment, Mz-ChA-1 cells were chosen due to their high motility and phenotype to grow as single cell monolayer. Cells were cultured to 100% confluency, treated with 15 ng/mL Hyper-IL-6, 100 ng/mL IL-6, 25 μg/mL Tocilizumab, 25 μg/

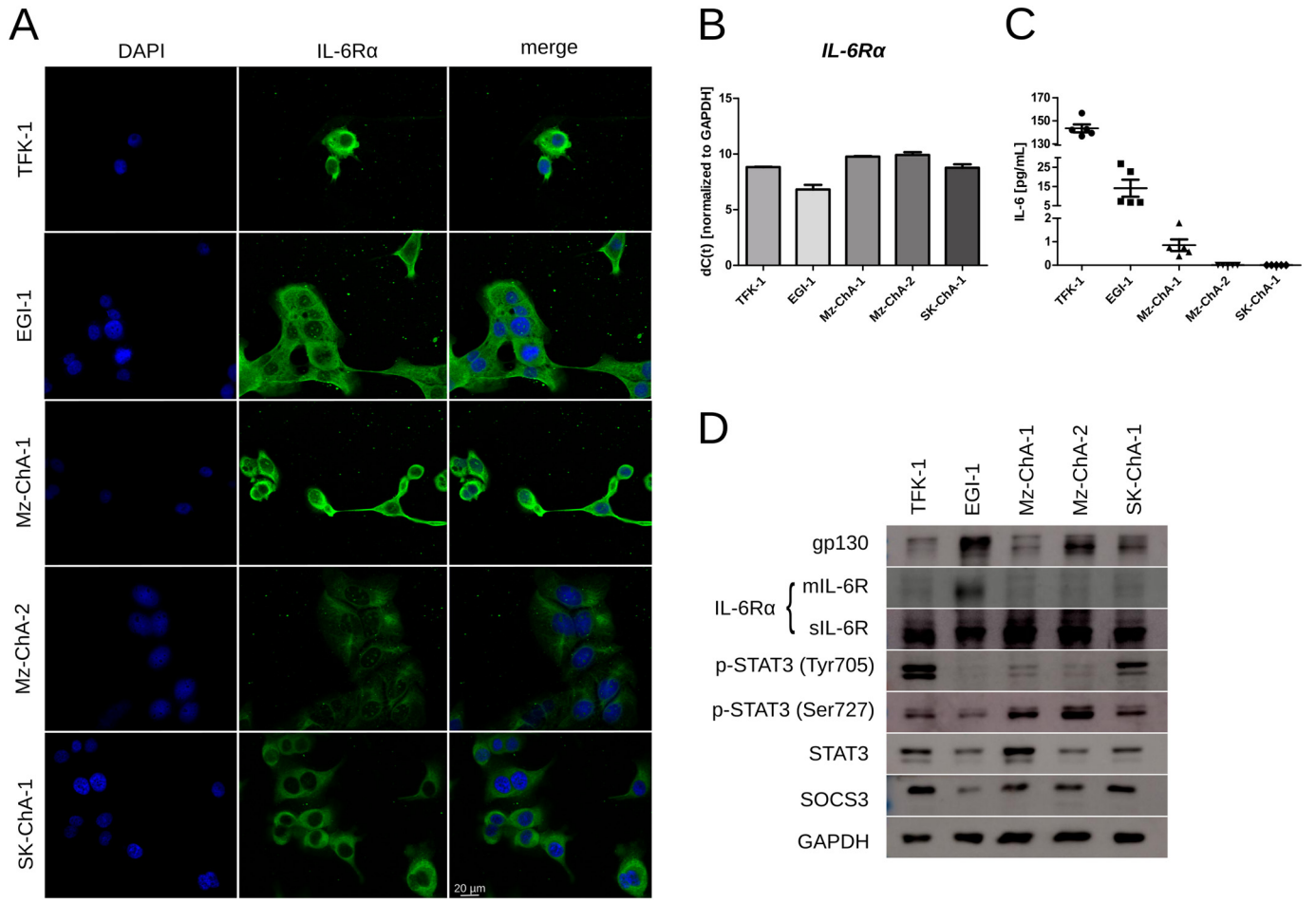

Fig. 3. Comparison of CCA cell lines regarding autocrine IL-6R signaling. (A) Visualization of the IL-6R (green) and the cell nucleus (blue) by immunofluorescence of five different CCA cell lines (bar = 20 µm). (B) Comparison of *IL-6Rα* gene expression in CCA cell lines by quantitative RT-PCR normalized to GAPDH. (C) Quantification of IL-6 in the cell culture supernatant after 24 h of serum starvation using ECLIA. (D) Representative immunoblot analysis of total cell line lysates regarding the expression of the soluble and membrane-bound IL-6R and its mediated signaling.

mL sgp130Fc or both, and a scratch assay was performed under serum starved conditions for 72 h. The blocking agents sgp130Fc and Tocilizumab led to a visible and significant ($p < 0.05$) increase in cell migration (Fig. 5A), whereas Hyper-IL-6 and IL-6 had only little effect. Opened wound area analysis (Fig. 5B) revealed a significantly ($p < 0.001$) enhanced migration of Mz-ChA-1 cells upon 25 µg/mL Tocilizumab treatment after 72 h.

3.7. Tocilizumab, sgp130Fc and IL-6 decrease cell viability

CCA cell lines (TKF-1 and Mz-ChA-2) were treated with various concentrations of all four compounds (Hyper-IL-6, IL-6, Tocilizumab and sgp130Fc) under serum starved conditions and viability was assessed using MTT assay. Hyper-IL-6 had no effect on cell viability within 72 h (Fig. 5C, Suppl. Fig. 2A). A significant decrease in cell viability was observed upon 15 ng/mL and 100 ng/mL IL-6 treatment (Fig. 5D, Suppl. Fig. 2B) after 72 h. The strongest reduction in viability (25%, $p < 0.001$) was detected after 72 h by blocking IL-6Rα using 25 µg/mL sgp130Fc (Fig. 5E, Suppl. Fig. 2C) or 25 µg/mL Tocilizumab (Fig. 5F, Suppl. Fig. 2D). This finding might be a result of the mitochondrial activity of STAT3.

3.8. Population doubling time and apoptosis are reduced by Tocilizumab, sgp130Fc and IL-6 in TFK-1 cells

To analyze changes in proliferation upon activation and inhibition of IL-6 classic signaling and trans-signaling in real time, xCELLigence technique was used (Fig. 6A–E and Suppl. Fig. 2E). Inhibition of IL-6Rα significantly ($p < 0.01$) increased the slope of the growth curve within 72 h in TFK-1 cells, thus reducing PDT under serum starved conditions by approximately 10 h (Fig. 6B–C). Mz-ChA-2 cells showed adverse effects except when the combination of Tocilizumab and sgp130Fc (Fig. 6D–E) was used. The most considerable difference of cell index was observed when cells were treated with 1 µg/mL sgp130Fc ($p < 0.001$), whereas IL-6 and Hyper-IL-6 showed no significant effect in both cell lines (Fig. 6A–B).

All four compounds (Hyper-IL-6, IL-6, Tocilizumab and sgp130Fc) affected apoptosis in TFK-1 cells. Hyper-IL-6 showed decreased apoptotic signals at lower concentrations ($p < 0.05$), whereas high Hyper-IL-6 concentration had no effect (Fig. 6F, Suppl. Fig. 2F) compared to control. The effect was the same when treated with IL-6 (Fig. 6G, Suppl. Fig. 2G). Blocking of IL-6Rα with 25 µg/mL Tocilizumab decreased apoptosis by 40% ($p < 0.001$) within 24 h (Fig. 6H, Suppl. Fig. 2I), and by 25% ($p < 0.001$) with 25 µg/mL sgp130Fc (Fig. 6I, Suppl. Fig. 2H).

3.9. Inhibition of the IL-6Rα by Tocilizumab or sgp130Fc induces a decrease of cells in the G2/M phase

To investigate changes in the cell cycle upon treatment, cells were treated under serum starved conditions, and cell cycle analysis was performed (Fig. 7A). The G0/G1 phase was not affected by treatment of any of the four compounds (Hyper-IL-6, IL-6, Tocilizumab and sgp13Fc;

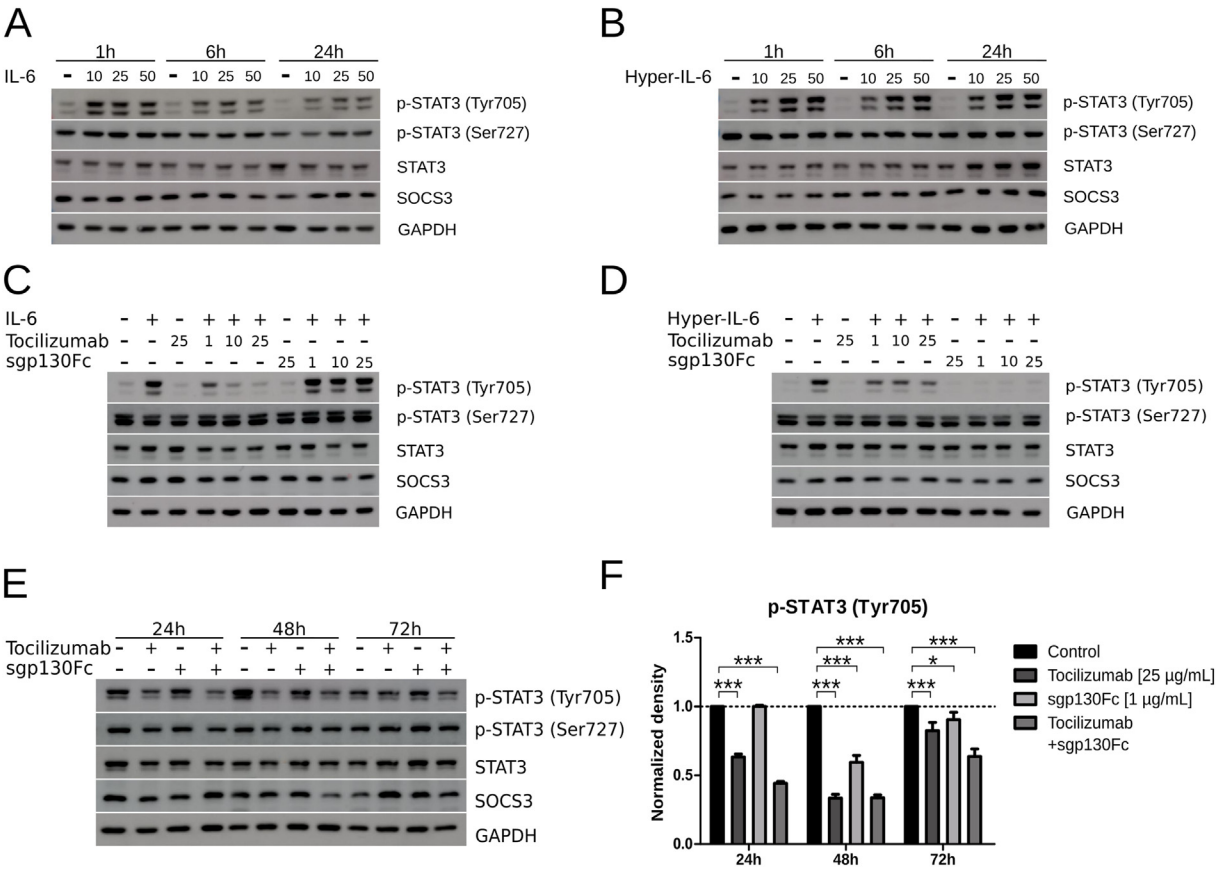

Fig. 4. Targeting IL-6Rα mediated signaling has a different impact on STAT3 phosphorylation in CCA cell lines. Mz-ChA-2 cells were treated with 10, 25 or 50 ng/mL (A) IL-6 or (B) Hyper-IL-6 for 1 h, 6 h and 24 h. Immunoblot of Mz-ChA-2 cells pretreated with 1, 10 or 25 µg/mL Tocilizumab or sgp130Fc for 6 h followed by 30 min incubation with (C) 100 ng/mL IL-6 or (D) 15 ng/mL Hyper-IL-6. (E) Analysis of STAT3 phosphorylation and SOCS3 after TFK-1 cells were treated with Tocilizumab (25 µg/mL), sgp130Fc (1 µg/mL) or in combination at 24 h, 48 h, and 72 h. (F) Densitometrical analysis by ImageJ of p-STAT3 (Tyr705) in TFK-1 cells after treatment with Tocilizumab (25 µg/mL) and/or sgp130Fc (1 µg/mL) normalized to solvent control. Bars represent mean ± SEM. *p < 0.05, **p < 0.01, ***p < 0.001. Statistical analysis: One-way ANOVA.

Fig. 7B and E). Tocilizumab and sgp130Fc showed the highest impact ($p < 0.05$) on cell cycle phase changes by increasing S-phase (Fig. 7C and G), and decreasing G2/M-phase (Fig. 7D and F; $p < 0.05$) after normalization to the control. Hyper-IL-6 and IL-6 did not induce significant cell cycle alterations in TFK-1 and Mz-ChA-2 cells (Fig. 7B–F). In summary, we conclude that IL-6 signaling represents a tumor supportive pathway in cholangiocarcinoma cells, and pharmacologic blockade of IL-6 signaling is dangerous in patients with biliary malignancies such as BTC.

4. Discussion

BTC is a silent cancer usually detected at advanced stage, where most patients are effected by unresectable tumors. At the time of manuscript preparation, 406 clinical trials (https://clinicaltrials.gov) were investigating effective treatment options. This is a significant number regarding the fact that little > 20.00 overall clinical trials are ongoing worldwide. The first targeted treatment using Sorafenib, an EGFR tyrosine kinase growth factor receptor inhibitor, displayed prolonged survival up to four years [43].

Our main conclusion is that IL-6 signaling predominantly promotes differentiation and is rather tumor supportive in CCA. As a consequence of the tumor supporting role of IL-6 in CCA, one should also evaluate carcinoma risk if IL-6Rα blockage treatment was performed, especially because liver damage is associated with higher CCA development.

Recent studies have demonstrated that the IL-6/IL-6R/gp130/STAT3 axis might play a role in BTC, but only the expression was correlated, and the implications for functional signaling were not studied. IL-6 expression correlates with survival of GBC patients, which is in line with our findings suggesting a tumor-supportive role of IL-6. We also confirmed the upregulation of IL-6 in GBC tissue [22] and the activation of STAT3 in CCA [10]. However, the biological consequence of different IL-6Rα signaling stimuli and their impact on tumor biology of BTC remains unclear. Our study is the first to examine the correlation between the expression of the IL-6Rα and prognosis in GBC providing insights into the cellular responses caused by IL-6 classic signaling and trans-signaling in CCA cell lines.

We found higher IL-6Rα expression and the correlation to longer GBC patients' overall survival. This finding was corroborated by *IL-6Rα* gene expression of CCA patients. IL-6Rα was shown to be downregulated in GBC tissue on protein and mRNA level. Identical findings have been reported in other solid tumors, such as ovarian [44] and breast cancer [45]. These findings indicate that not only IL-6 but also IL-6Rα plays an important role in several tumor entities. The *ADAM17* gene expression and the downregulation of the mIL-6R might constitute a possible shedding mechanism in GBC. This process could lead to the stimulation of hepatocytes around the bile ducts. Furthermore, it can activate Kupffer cells, leading to a feedback loop activation. IL-6 trans-signaling is ten times more potent than IL-6, so the CCA cells are able to create an inflammatory milieu in a fraction of CCAs facilitating tissue remodeling or wound healing. Therefore, it is of interest for further studies to analyze GBC or BTC patients in general, for the concentration of circulating sIL-6R and the soluble form of gp130. Moreover, analysis of the tumor microenvironment may clarify the origin of soluble

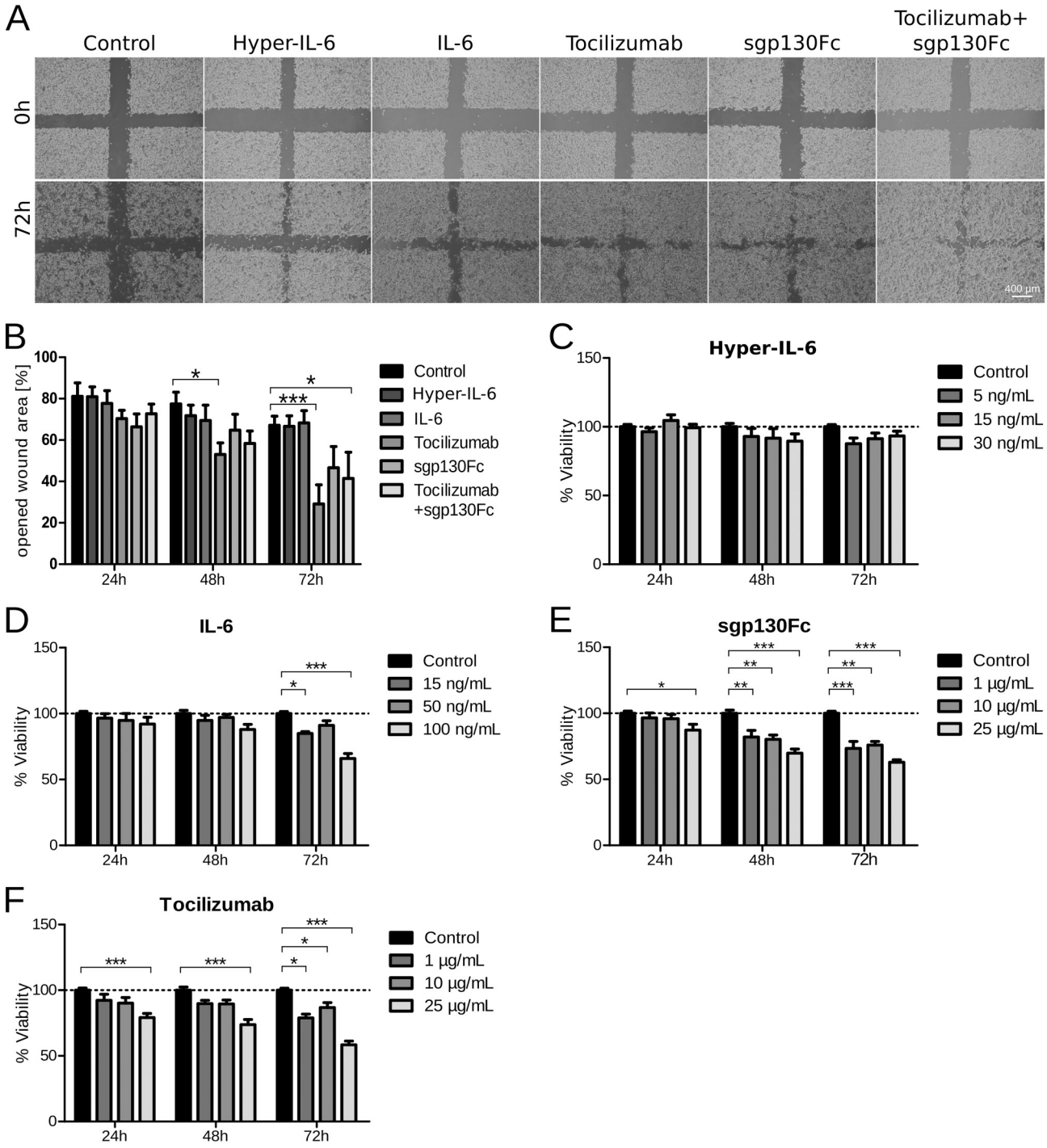

Fig. 5. Inhibition of the IL-6Rα leads to enhanced cell migration and reduced viability in CCA cell lines. Mz-ChA-1 cells were cultivated to 100% confluency, wounded, treated and wound closure was assessed over 72 h. (A) Representative pictures of start and endpoint (72 h) of the migration assay *in vitro*. (scale bar = 400 µm). (B) Calculated percentage of opened wound area by TScratch software upon treatment over time. MTT assay analyzing the viability of TFK-1 cells treated with (C) Hyper-IL-6, (D) IL-6, (E) sgp130Fc and (F) Tocilizumab over 72 h normalized to vehicle control. Bars represent mean ± SEM. *p < 0.05, **p < 0.01, *** p < 0.001. Statistical test: one-way ANOVA. Each experiment was performed three independent times.

receptors in BTC and might therefore represent a possible immunotherapeutic target.

Our study revealed that STAT3 is downregulated at the protein level in GBC, but upregulated at the mRNA level. However, ratios of p-STAT3 (Tyr705) and total STAT3 remain unaffected, indicating activation of STAT3 in GBC and non-neoplastic gallbladder tissues.

Overall, our results are in line with those obtained by examining the high number of FFPE material immunostaining results. We conclude that a general downregulation of the IL-6Rα takes place in BTC presumably due to tumor suppressive function. However, to verify this conclusion, CCA tissues have to be analyzed.

Several studies have reported differences in the activation of STAT3 caused by IL-6 classic signaling and trans-signaling. Compared to IL-6 in CCA cell lines, Hyper-IL-6 induced a prolonged and stronger tyrosine phosphorylation of STAT3. This result is consistent with that reported by Holmer et al. [46], describing the effect of Hyper-IL-6 in colorectal

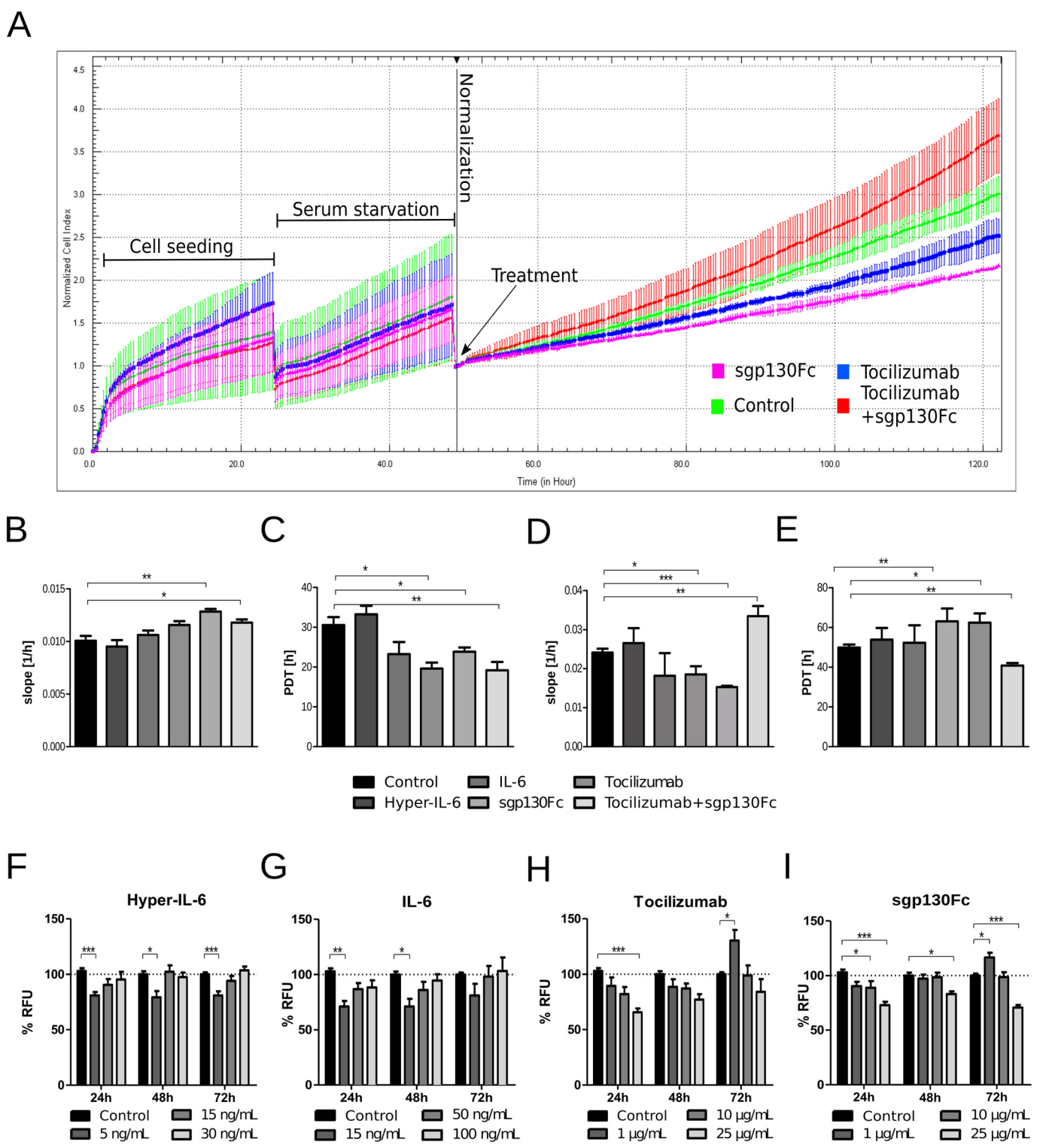

Fig. 6. Inhibition of the IL-6Rα in CCA cell lines leads to increased proliferation and decreased apoptotic signals. (A) Representative growth curve measured using xCELLigence for the treatment Tocilizumab (25 µg/mL), sgp130Fc (1 µg/mL) or in combination. (B–E) Calculated slope in the log-phase of the growth curve and resulting population doubling time (PDT) of (B–C) TFK-1 and (D–E) Mz-ChA-2 cells treated with Hyper-IL-6 (15 ng/mL), IL-6 (100 ng/mL), Tocilizumab (25 µg/mL), sgp130Fc (1 µg/mL) or in combination. (F–I) Apoptotic signals measured by YoPro-1 fluorescence upon treatment with indicated concentrations of Hyper-IL-6, IL-6, Tocilizumab and sgp130Fc over 72 h normalized to control. Bars represent mean ± SEM. *p < 0.05, **p < 0.01, ***p < 0.001. Statistical test: one-way ANOVA. Each experiment was performed three independent times.

cancer cell lines, or Sun et al. [47], who also demonstrated differences in STAT3 phosphorylation upon treatment with IL-6 and Hyper-IL-6 in primary hippocampal neurons. Interestingly, it was shown that IL-6 was rapidly internalized in hepatocytes, possibly causing a decrease of the p-STAT3 (Tyr705) signal over time [48]. This effect might explain the differences in STAT3 phosphorylation in CCA cell lines by IL-6 internalization. However, Hyper-IL-6 did not induce remarkable differences in the examined cellular responses, including the expression of SOCS3.

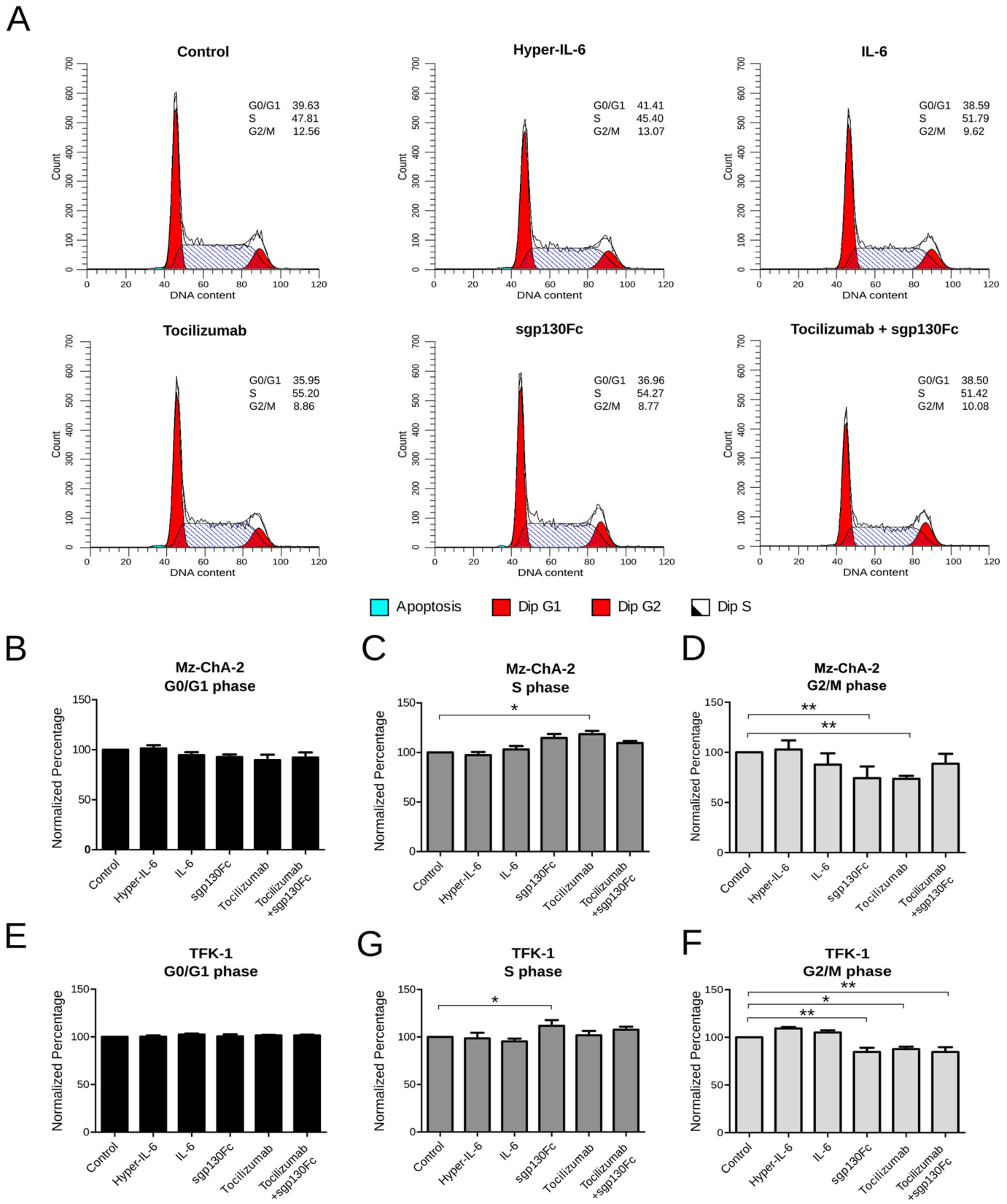

Fig. 7. IL-6Rα blockage changes the cell cycle profiles in CCA cell lines. Mz-ChA-2 cells upon serum starvation and cell cycle analysis 72 h after treatment with Hyper-IL-6 (15 ng/mL), IL-6 (100 ng/mL), sgp130Fc (1 μg/mL), Tocilizumab (25 μg/mL) or combined treatment with Tocilizumab and sgp130Fc measured by flow cytometry. (A) Representative graphs for cell cycle measurement followed by ModFIT LT software version 5.0 analysis. (B–F) Percentage of Mz-ChA-2 cells and TFK-1 cells in G0/G1-phase, S-phase and G2/M-phase normalized to control. Bars represent mean ± SEM. *p > 0.05, **p > 0.01, *** p < 0.001. Statistical test: one-way ANOVA. Each experiment was performed three independent times.

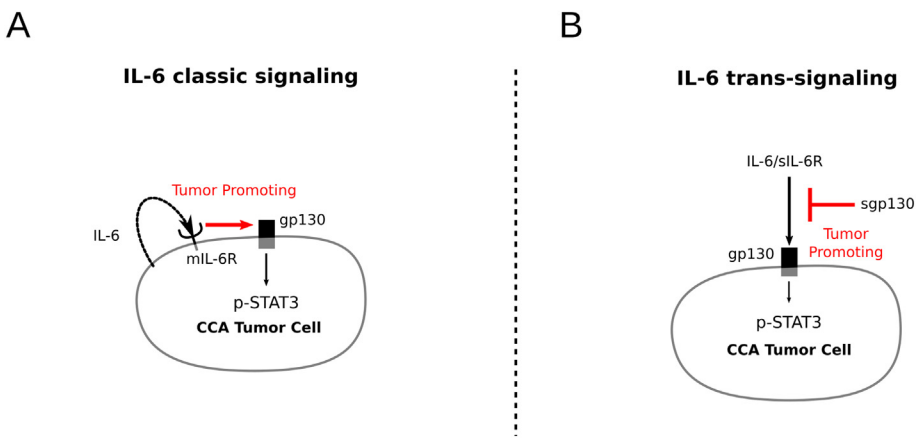

Fig. 8. Tumor-promoting effects of IL-6 classic and trans-signaling in CCA *in vitro*. (A) Effects of autocrine IL-6 stimulation (activation of classic IL-6 signaling) in CCA revealed to be tumor promoting. (B) Schematic overview of IL-6 trans-signaling. Blocking IL-6 trans-signaling *via* soluble gp130 shows tumor-promoting effects *in vitro*.

This led us to the suggestion that activation of STAT3 by IL-6 trans-signaling may only play a minor role in CCA, but the strong serine phosphorylation of STAT3 was persistent in CCA and independent of IL-6 signaling. This suggests that mitochondrial STAT3 activity triggered by serine phosphorylation of STAT3 could play an essential role in CCA. Moreover, the reduced mitochondrial activity (cell viability) found by IL-6R blockage highlights the potential role of mitochondrial STAT3 in CCA cell lines [49,50].

IL-6 was found to impact CCA in many ways. For instance, stable overexpression of IL-6 in Mz-ChA-1 cells increased transformed cell growth and tumor growth *in vivo* [51]. The same research group reported that exogenous IL-6 increased the proliferation of CCA cells [52]. Our study demonstrated that the proliferation of CCA cell lines is increased upon IL-6 treatment. Interestingly, analysis of the metabolic activity upon IL-6 treatment revealed a decrease in viability after 72 h without affecting cell migration and cell cycle distribution. Moreover, only low dosages of IL-6 decreased apoptotic signals. This may indicate tumor promoting activities of IL-6 in CCA *in vitro*.

IL-6Rα blockage with Tocilizumab, an immunosuppressive drug mainly used for the treatment of rheumatoid arthritis, is becoming important for the treatment of various malignancies, including cancer. Treatment of non-small cell lung cancer cells with Tocilizumab induced a sub-G1 arrest [53]. In chronic lymphocytic leukemia, Tocilizumab increased the number of G1 phase cells, hence promoting re-entry into the cell cycle [54]. Our study revealed that Tocilizumab affects S and G2/M phase cells in CCA cell lines, suggesting highly proliferative cells. We also found an increase of PDT in Tocilizumab-treated TFK-1 cells, and in combination with sgp130Fc for Mz-ChA-2 cells. In TFK-1 cells, Tocilizumab decreased tyrosine phosphorylation of STAT3. However, STAT3 is still activated, which may be due to the autocrine secretion of IL-6 in TFK-1 cells.

The differentiation between IL-6 classic signaling and trans-signaling is a subject of growing interest [42]. Therefore, Tocilizumab was compared with sgp130Fc, which specifically blocks IL-6 trans-signaling without affecting the classic signaling of IL-6. Blocking IL-6 trans-signaling by sgp130Fc increased cell migration, and after 48 h, the constitutive STAT3 phosphorylation in TFK-1 cells was decreased. Taken together, sgp130Fc had similar effects on cellular processes like Tocilizumab. This indicates that the observed effects induced by Tocilizumab may be due to the blocking of the soluble IL-6R.

In conclusion, we found that IL-6Rα is a novel prognostic factor for overall survival in GBC. Our results show that the role played by activation of classic IL-6 signaling is superior to that played by the activation of IL-6 trans-signaling. Treatment with Tocilizumab and sgp130Fc revealed similar advantage for CCA tumor cells. Thus, blocking of IL-6 trans-signaling might promote tumor growth and also interference of IL-6 signaling in HCC could be dangerous (Fig. 8).

Transparency document

The Transparency document associated with this article can be found, in online version.

Acknowledgments

This study was supported by the research scholarship of the Medical University of Graz, the FFG (# 415 854452) and was carried out in course of the Doctoral School "General and Clinical Pathophysiology" of the Medical University of Graz. We thank Carolin Lackner for her valuable feedback, Margit Gogg-Kammerer for her technical support, and Paul Baran as well as Juergen Scheller for providing the IL-6Rα antibody.

Author contributions

F.K., N. G.-S., S.K., C.G., P.F., S. R.-J., B.R., R.M. and J.H. designed and planned the study. A.M. B.-T. analyzed the TCGA database. E.H. stained and E.H. and J.H. scored the IHC. R.R. and J.P. evaluated the TMA data. F.K., C.W., N.G.-S., T.N., S.K., A.O., H.M. and A.S. performed the biochemical analysis. M.T., A.A., C.G., S-R.-J., B.R., N.Y.P., S.L. and J.H. provided resources and tissue. F.K. wrote the manuscript. All authors discussed the data during the course of the project, revised and approved the final manuscript. J.H. and R.M. acquired funding for conducting the entire study.

Conflicts of interest

S.R.-J. is a shareholder of the CONARIS Research Institute AG (Kiel, Germany), which develops soluble glycoprotein 130 fusion proteins (sgp130Fcs) as therapeutics for inflammatory diseases. All other authors declare no conflicts of interest.

Appendix A. Supplementary data

Supplementary data to this article can be found online at https://doi.org/10.1016/j.bbadis.2018.11.006.

References

[1] A. Nakeeb, H.A. Pitt, T.A. Sohn, J. Coleman, R.A. Abrams, S. Piantadosi, et al., Cholangiocarcinoma. A spectrum of intrahepatic, perihilar, and distal tumors, Ann. Surg. 224 (1996) 463–473, https://doi.org/10.1097/01.sla.0000251366.62632.d3 (discussion 473–5).

[2] H.R. Shin, J.K. Oh, E. Masuyer, M.P. Curado, V. Bouvard, Y.Y. Fang, et al., Epidemiology of cholangiocarcinoma: an update focusing on risk factors, Cancer Sci. 101 (2010) 579–585, https://doi.org/10.1111/j.1349-7006.2009.01458.x.

[3] S. Tazuma, G. Kajiyama, Carcinogenesis of malignant lesions of the gall bladder: the impact of chronic inflammation and gallstones, Langenbeck's Arch. Surg. 386

(2001) 224–229, https://doi.org/10.1007/s004230100220.
[4] T. Rustagi, C.A. Dasanu, Risk factors for gallbladder cancer and cholangiocarcinoma: similarities, differences and updates, J. Gastrointest. Cancer 43 (2012) 137–147, https://doi.org/10.1007/s12029-011-9284-y.
[5] Y. Xu, N.J. Kershaw, C.S. Luo, P. Soo, M.J. Pocock, P.E. Czabotar, et al., Crystal structure of the entire ectodomain of gp130: insights into the molecular assembly of the tall cytokine receptor complexes, J. Biol. Chem. 285 (2010) 21214–21218, https://doi.org/10.1074/jbc.C110.129502.
[6] E.T. Keller, J. Wanagat, W.B. Ershler, Molecular and cellular biology of interleukin-6 and its receptor, Front. Biosci. 1 (1996) d340–d357.
[7] D.R. Hodge, E.M. Hurt, W.L. Farrar, The role of IL-6 and STAT3 in inflammation and cancer, Eur. J. Cancer 41 (2005) 2502–2512, https://doi.org/10.1016/j.ejca.2005.08.016.
[8] H. Yu, D. Pardoll, R. Jove, STATs in cancer inflammation and immunity: a leading role for STAT3, Nat. Rev. Cancer 9 (2009) 798–809, https://doi.org/10.1038/nrc2734.
[9] H. Nivarthi, C. Gordziel, M. Themanns, N. Kramer, M. Eberl, B. Rabe, et al., The ratio of STAT1 to STAT3 expression is a determinant of colorectal cancer growth, Oncotarget 7 (2016) 51096–51106, https://doi.org/10.18632/oncotarget.9315.
[10] H. Dokduang, A. Techasen, N. Namwat, N. Khuntikeo, C. Pairojkul, Y. Murakami, et al., STATs profiling reveals predominantly-activated STAT3 in cholangiocarcinoma genesis and progression, J. Hepatobiliary Pancreat. Sci. 21 (2014) 767–776, https://doi.org/10.1002/jhbp.131.
[11] T. Taga, IL6 signalling through IL6 receptor and receptor-associated signal transducer, gp130, Res. Immunol. 143 (1992) 737–739.
[12] A. Mackiewicz, H. Schooltink, P.C. Heinrich, S. Rose-John, Complex of soluble human IL-6-receptor/IL-6 up-regulates expression of acute-phase proteins, J. Immunol. 149 (1992) 2021–2027.
[13] C. Garbers, N. Jänner, A. Chalaris, M.L. Moss, D.M. Floss, D. Meyer, et al., Species specificity of ADAM10 and ADAM17 proteins in interleukin-6 (IL-6) trans-signaling and novel role of ADAM10 in inducible IL-6 receptor shedding, J. Biol. Chem. 286 (2011) 14804–14811, https://doi.org/10.1074/jbc.M111.229393.
[14] E.M. Briso, O. Dienz, M. Rincon, Cutting edge: soluble IL-6R is produced by IL-6R ectodomain shedding in activated CD4 T cells, J. Immunol. 180 (2008) 7102–7106 (doi:180/11/7102 [pii]).
[15] V. Matthews, B. Schuster, S. Schütze, I. Bussmeyer, A. Ludwig, C. Hundhausen, et al., Cellular cholesterol depletion triggers shedding of the human interleukin-6 receptor by ADAM10 and ADAM17 (TACE), J. Biol. Chem. 278 (2003) 38829–38839, https://doi.org/10.1074/jbc.M210584200.
[16] S. Riethmueller, P. Somasundaram, J.C. Ehlers, C.W. Hung, C.M. Flynn, J. Lokau, et al., Proteolytic origin of the soluble human IL-6R in vivo and a decisive role of *N*-glycosylation, PLoS Biol. 15 (2017), https://doi.org/10.1371/journal.pbio.2000080.
[17] P. Prayong, E. Mairiang, C. Pairojkul, Y. Chamgramol, P. Mairiang, V. Bhudisawasdi, et al., An interleukin-6 receptor polymorphism is associated with opisthorchiasis-linked cholangiocarcinoma risk in Thailand, Asian Pac. J. Cancer Prev. 15 (2014) 5443–5447, https://doi.org/10.7314/APJCP.2014.15.13.5443.
[18] H. Isomoto, J.L. Mott, S. Kobayashi, N.W. Werneburg, S.F. Bronk, S. Haan, et al., Sustained IL-6/STAT-3 signaling in cholangiocarcinoma cells due to SOCS-3 epigenetic silencing, Gastroenterology 132 (2007) 384–396, https://doi.org/10.1053/j.gastro.2006.10.037.
[19] Y.K. Cheon, Y.D. Cho, J.H. Moon, J.Y. Jang, Y.S. Kim, Y.S. Kim, et al., Diagnostic utility of interleukin-6 (IL-6) for primary bile duct cancer and changes in serum IL-6 levels following photodynamic therapy, Am. J. Gastroenterol. 102 (2007) 2164–2170, https://doi.org/10.1111/j.1572-0241.2007.01403.x.
[20] J.B. Andersen, S.S. Thorgeirsson, A perspective on molecular therapy in cholangiocarcinoma: present status and future directions, Hepatic Oncol. 1 (2014), https://doi.org/10.1126/scisignal.2001449.Engineering (22 pages).
[21] J.S. Goydos, A.M. Brumfield, E. Frezza, A. Booth, M.T. Lotze, S.E. Carty, Marked elevation of serum interleukin-6 in patients with cholangiocarcinoma: validation of utility as a clinical marker, Ann. Surg. 227 (1998) 398–404, https://doi.org/10.1097/00000658-199803000-00012.
[22] M. Zhang, W. Gong, Y. Zhang, Y. Yang, D. Zhou, M. Weng, et al., Expression of interleukin-6 is associated with epithelial-mesenchymal transition and survival rates in gallbladder cancer, Mol. Med. Rep. 11 (2015) 3539–3546, https://doi.org/10.3892/mmr.2014.3143.
[23] H. Wehbe, R. Henson, F. Meng, J. Mize-Berge, T. Patel, Interleukin-6 contributes to growth in cholangiocarcinoma cells by aberrant promoter methylation and gene expression, Cancer Res. 66 (2006) 10517–10524, https://doi.org/10.1158/0008-5472.CAN-06-2130.
[24] M. Lesina, M.U. Kurkowski, K. Ludes, S. Rose-John, M. Treiber, G. Klöppel, et al., Stat3/Socs3 activation by IL-6 transsignaling promotes progression of pancreatic intraepithelial neoplasia and development of pancreatic cancer, Cancer Cell 19 (2011) 456–469, https://doi.org/10.1016/j.ccr.2011.03.009.
[25] J. Bergmann, M. Müller, N. Baumann, M. Reichert, C. Heneweer, J. Bolik, et al., IL-6 trans-signaling is essential for the development of hepatocellular carcinoma in mice, Hepatology 65 (2017), https://doi.org/10.1002/hep.28874.
[26] R.M. McLoughlin, B.J. Jenkins, D. Grail, A.S. Williams, C.A. Fielding, C.R. Parker, et al., IL-6 trans-signaling via STAT3 directs T cell infiltration in acute inflammation, Proc. Natl. Acad. Sci. 102 (2005) 9589–9594, https://doi.org/10.1073/pnas.0501794102.
[27] S. Rose-John, Il-6 trans-signaling via the soluble IL-6 receptor: importance for the proinflammatory activities of IL-6, Int. J. Biol. Sci. 8 (2012) 1237–1247, https://doi.org/10.7150/ijbs.4989.
[28] M.A. Nowell, A.S. Williams, S.A. Carty, J. Scheller, A.J. Hayes, G.W. Jones, et al., Therapeutic targeting of IL-6 trans signaling counteracts STAT3 control of experimental inflammatory arthritis, J. Immunol. 182 (2009) 613–622, https://doi.org/10.4049/jimmunol.182.1.613.
[29] H. Schuett, R. Oestreich, G.H. Waetzig, W. Annema, M. Luchtefeld, A. Hillmer, et al., Transsignaling of interleukin-6 crucially contributes to atherosclerosis in mice, Arterioscler. Thromb. Vasc. Biol. 32 (2012) 281–290, https://doi.org/10.1161/ATVBAHA.111.229435.
[30] T. Barkhausen, T. Tschernig, P. Rosenstiel, M. Van Griensven, R.P. Vonberg, M. Dorsch, et al., Selective blockade of interleukin-6 trans-signaling improves survival in a murine polymicrobial sepsis model, Crit. Care Med. 39 (2011) 1407–1413, https://doi.org/10.1097/CCM.0b013e318211ff56.
[31] S.M. Kessler, E. Lederer, S. Laggai, N. Golob-Schwarzl, K. Hosseini, J. Petzold, et al., IMP2/IGF2BP2 expression, but not IMP1 and IMP3, predicts poor outcome in patients and high tumor growth rate in xenograft models of gallbladder cancer, Oncotarget 8 (2017) 89736–89745, https://doi.org/10.18632/oncotarget.21116.
[32] N. Golob-Schwarzl, S. Krassnig, A.M. Toeglhofer, Y.N. Park, M. Gogg-Kamerer, K. Vierlinger, et al., New liver cancer biomarkers: PI3K/AKT/mTOR pathway members and eukaryotic translation initiation factors, Eur. J. Cancer 83 (2017) 56–70, https://doi.org/10.1016/j.ejca.2017.06.003.
[33] N. Golob-Schwarzl, C. Schweiger, C. Koller, S. Krassnig, M. Gogg-kamerer, N. Gantenbein, et al., Separation of Low and High Grade Colon and Rectum Carcinoma by Eukaryotic Translation Initiation Factors 1, 5 and 6, 8 (2017), pp. 101224–101243, https://doi.org/10.18632/oncotarget.20642.
[34] C.L. Andersen, J.L. Jensen, T.F. Ørntoft, Normalization of real-time quantitative reverse transcription-PCR data: a model-based variance estimation approach to identify genes suited for normalization, applied to bladder and colon cancer data sets, Cancer Res. 64 (2004) 5245–5250, https://doi.org/10.1158/0008-5472.CAN-04-0496.
[35] K.J. Livak, T.D. Schmittgen, Analysis of relative gene expression data using real-time quantitative PCR and the 2(−Delta Delta C(T)) method, Methods 25 (2001) 402–408.
[36] B. Goeppert, C. Konermann, C.R. Schmidt, O. Bogatyrova, L. Geiselhart, C. Ernst, et al., Global alterations of DNA methylation in cholangiocarcinoma target the Wnt signaling pathway, Hepatology 59 (2014) 544–554, https://doi.org/10.1002/hep.26721.
[37] M. Fischer, J. Goldschmitt, C. Peschel, J.P.G. Brakenhoff, K.J. Kallen, A. Wollmer, et al., A bioactive designer cytokine for human hematopoietic progenitor cell expansion, Nat. Biotechnol. 15 (1997) 142–145, https://doi.org/10.1038/nbt0297-142.
[38] M. Van Dam, J. Müllberg, H. Schooltink, T. Stoyan, J.P.J. Brakenhoff, L. Graeve, et al., Structure-function analysis of interleukin-6 utilizing human/murine chimeric molecules: involvement of two separate domains in receptor binding, J. Biol. Chem. 268 (1993) 15285–15290.
[39] S. Tenhumberg, G.H. Waetzig, A. Chalaris, B. Rabe, D. Seegert, J. Scheller, et al., Structure-guided optimization of the interleukin-6 trans-signaling antagonist sgp130, J. Biol. Chem. 283 (2008) 27200–27207, https://doi.org/10.1074/jbc.M803694200.
[40] T. Jostock, J. Müllberg, S. Özbek, R. Atreya, G. Blinn, N. Voltz, et al., Soluble gp130 is the natural inhibitor of soluble interleukin-6 receptor transsignaling responses, Eur. J. Biochem. 268 (2001) 160–167, https://doi.org/10.1046/j.1432-1327.2001.01867.x.
[41] T. Gebaeck, M.M.P. Schulz, P. Koumoutsakos, M. Detmar, TScratch: a novel and simple software tool for automated analysis of monolayer wound healing assays, Biotechniques 46 (2009) 265–274, https://doi.org/10.2144/000113083.
[42] D. Schmidt-Arras, S. Rose-John, IL-6 pathway in the liver: from physiopathology to therapy, J. Hepatol. 64 (2016) 1403–1415, https://doi.org/10.1016/j.jhep.2016.02.004.
[43] H.R. Chakunta, R. Sunderkrishnan, M.A. Kaplan, R. Mostofi, Cholangiocarcinoma: treatment with sorafenib extended life expectancy to greater than four years, J. Gastrointest. Oncol. 4 (2013), https://doi.org/10.3978/j.issn.2078-6891.2013.031.
[44] Q. Chen, B. Xu, L. Lan, D. Yang, M. Yang, J. Jiang, et al., High mRNA expression level of IL-6R was associated with better prognosis for patients with ovarian cancer: a pooled meta-analysis, Sci. Rep. 7 (2017) 8769, https://doi.org/10.1038/s41598-017-09333-8.
[45] A. Karczewska, S. Nawrocki, D. Bręborowicz, V. Filas, A. Mackiewicz, Expression of interleukin-6, interleukin-6 receptor, and glycoprotein 130 correlates with good prognoses for patients with breast carcinoma, Cancer 88 (2000) 2061–2071, https://doi.org/10.1002/(SICI)1097-0142(20000501)88:9<2061::AID-CNCR12>3.0.CO;2-O.
[46] R. Holmer, G.H. Wätzig, S. Tiwari, S. Rose-John, H. Kalthoff, Interleukin-6 trans-signaling increases the expression of carcinoembryonic antigen-related cell adhesion molecules 5 and 6 in colorectal cancer cells, BMC Cancer 15 (2015) 975, https://doi.org/10.1186/s12885-015-1950-1.
[47] Y. Sun, P. März, U. Otten, J. Ge, S. Rose-John, The effect of gp130 stimulation on glutamate-induced excitotoxicity in primary hippocampal neurons, Biochem. Biophys. Res. Commun. 295 (2002) 532–539, https://doi.org/10.1016/S0006-291X(02)00706-4.
[48] E. Dittrich, S. Rose-John, C. Gerhartz, J. Müllberg, T. Stoyan, K. Yasukawa, et al., Identification of a region within the cytoplasmic domain of the interleukin-6 (IL-6) signal transducer gp130 important for ligand-induced endocytosis of the IL-6 receptor, J. Biol. Chem. 269 (1994) 19014–19020, https://doi.org/10.1111/j.1749-6632.1995.tb32350.x.
[49] D.J. Gough, A. Corlett, K. Schlessinger, J. Wegrzyn, A.C. Larner, D.E. Levy, Mitochondrial STAT3 supports RasDependent oncogenic transformation, Science 324 (2009) 1713–1716, https://doi.org/10.1126/science.1171721.
[50] R. Yang, M. Rincon, Mitochondrial Stat3, the need for design thinking, Int. J. Biol. Sci. 12 (2016) 532–544, https://doi.org/10.7150/ijbs.15153.

[51] F. Meng, Y. Yamagiwa, Y. Ueno, T. Patel, Over-expression of interleukin-6 enhances cell survival and transformed cell growth in human malignant cholangiocytes, J. Hepatol. 44 (2006) 1055–1065, https://doi.org/10.1016/j.jhep.2005.10.030.
[52] J. Park, L. Tadlock, G.J. Gores, T. Patel, Inhibition of interleukin 6-mediated mitogen-activated protein kinase activation attenuates growth of a cholangiocarcinoma cell line, Hepatology 30 (1999) 1128–1133, https://doi.org/10.1002/hep.510300522.
[53] N.H. Kim, S.K. Kim, D.S. Kim, D. Zhang, J.A. Park, H. Yi, et al., Anti-proliferative action of IL-6r-targeted antibody tocilizumab for non-small cell lung cancer cells, Oncol. Lett. 9 (2015) 2283–2288, https://doi.org/10.3892/ol.2015.3019.
[54] F.T. Liu, L. Jia, P. Wang, T. Farren, H. Li, X. Hao, et al., CD126 and targeted therapy with tocilizumab in chronic lymphocytic leukemia, Clin. Cancer Res. 22 (2016) 2462–2469, https://doi.org/10.1158/1078-0432.CCR-15-1139.
[55] A. Chalaris, B. Rabe, K. Paliga, H. Lange, T. Laskay, C.A. Fielding, et al., Apoptosis is a natural stimulus of IL6R shedding and contributes to the proinflammatory trans-signaling function of neutrophils, Blood 110 (2007) 1748–1755, https://doi.org/10.1182/blood-2007-01-067918.